Human axons contain at least five types of voltage-dependent potassium channel

Gordon Reid, Andreas Scholz*, Hugh Bostock and Werner Vogel*

*Sobell Department of Neurophysiology, Institute of Neurology, Queen Square, London WC1N 3BG, UK and *Physiologisches Institut, Justus-Liebig-Universität Giessen, Aulweg 129, 35392 Giessen, Germany*

(Received 22 February 1999; accepted after revision 6 May 1999)

1. We investigated voltage-gated potassium channels in human peripheral myelinated axons; apart from the I, S and F channels already described in amphibian and rat axons, we identified at least two other channel types.

2. The I channel activated between −70 and −40 mV, and inactivated very slowly (time constant 13·1 s at −40 mV). It had two gating modes: the dominant ('noisy') mode had a conductance of 30 pS (inward current, symmetrical 155 mM K^+) and a deactivation time constant (τ) of 25 ms (−80 mV); it accounted for most (~50–75%) of the macroscopic K^+ current in large patches. The secondary ('flickery') gating mode had a conductance of 22 pS, and showed bi-exponential deactivation ($\tau = 16$ and 102 ms; −80 mV); it contributed part of the slow macroscopic K^+ current.

3. The I channel current was blocked by 1 μM α-dendrotoxin (DTX); we also observed two other DTX-sensitive K^+ channel types (40 pS and 25 pS). The S and F channels were not blocked by 1 μM DTX.

4. The conductance of the S channel was 7–10 pS, and it activated at slightly more negative potentials than the I channel; its deactivation was slow ($\tau = 41{\cdot}7$ ms at −100 mV). It contributed a second component of the slow macroscopic K^+ current.

5. The F channel had a conductance of 50 pS; it activated at potentials between −40 and +40 mV, deactivated very rapidly ($\tau = 1{\cdot}4$ ms at −100 mV), and inactivated rapidly ($\tau = 62$ ms at +80 mV). It accounted for the fast-deactivating macroscopic K^+ current and partly for fast K^+ current inactivation.

6. We conclude that human and rat axonal K^+ channels are closely similar, but that the correspondence between K^+ channel types and the macroscopic currents usually attributed to them is only partial. At least five channel types exist, and their characteristics overlap to a considerable extent.

Myelinated axons have been shown to contain at least three types of potassium current activated by depolarization: two fast currents, labelled I_{Kf1} and I_{Kf2}, and one slow current, labelled I_{Ks}. These have been identified in frog nodes of Ranvier (Dubois, 1981) and internodes (Grissmer, 1986), and similar currents appear to be present in rat axons, albeit with a different spatial distribution (Röper & Schwarz, 1989; Corrette *et al.* 1991). Single-channel recordings in myelinated axons from *Xenopus* (Jonas *et al.* 1989) and rat (Safronov *et al.* 1993) reveal three types of voltage-dependent K^+ channel: the F (fast) channel, which activates rapidly over a broad range of relatively positive membrane potentials, and deactivates rapidly; the S (slow) channel, which activates at more negative potentials and has slower kinetics; and the I (intermediate) channel, which activates at similar potentials to the S channel, and has kinetics intermediate between those of the other two types. It has been suggested that these channels underlie the I_{Kf2}, I_{Ks} and I_{Kf1} currents, respectively (Jonas *et al.* 1989). Experiments in undissected axons allow conclusions to be drawn about the likely functions of these currents: the fast K^+ currents I_{Kf1} and I_{Kf2} appear to limit repetitive activity after a single impulse; accommodation is influenced by I_{Kf1} and I_{Ks}; and I_{Ks} is also important for spike-frequency adaptation (Baker *et al.* 1987; Poulter *et al.* 1989). The resting potential is probably determined in large part by the internodal I_{Ks} and I_{Kf1} conductances, which are active near the resting potential (Grafe *et al.* 1994). In mammals, the nodal fast K^+ conductances are small and their activation plays no significant part in repolarization after the action potential (Chiu *et al.* 1979). The field has been reviewed by Vogel & Schwarz (1995).

Although human axons generate action potentials in a similar way to those of other species, and human nodes of Ranvier contain ionic currents with similar properties to those in rat and amphibian axons (Schwarz *et al.* 1995), *in vivo* recordings reveal electrophysiological differences between human and rat axons which suggest different populations of voltage-gated K^+ channels (Bostock & Baker, 1988). Such species differences would have important consequences, because axonal K^+ channels are one target for symptomatic treatment of demyelinating diseases like multiple sclerosis (Davis *et al.* 1990; Schwid *et al.* 1997). We therefore investigated human axonal ion channels with the patch-clamp technique, and our initial impression was that channels in rat and human axons are similar (Scholz *et al.* 1993). We have now characterized in detail the properties of single K^+ channels in human axons, and find close quantitative similarities with those in rat and amphibian axons; the species differences observed *in vivo* therefore do not result from substantial differences in the single-channel properties. Our results do not support a simple classification of axonal K^+ channels into three distinct types responsible for the three macroscopic currents described above: at least five types are present, and their kinetic properties show a substantial degree of overlap.

METHODS

Preparation

The source of human nerve was excess donor material from nerve-graft operations, which would otherwise have been discarded. The procedure was approved by the ethical committee of the Institute of Neurology and the National Hospital for Neurology and Neurosurgery. The age of the patients was 17–48 years. Short pieces (< 5 cm) of nerve were transferred directly from the patient into sterile tissue culture medium (Dulbecco's modified Eagle's medium (DMEM)–Ham's F12; Gibco, Paisley, Scotland), which had been saturated with 95 % O_2–5 % CO_2, and were transported to the laboratory at the Institute of Neurology by courier; nerves arrived within 2 h of removal and were thereafter stored at 10 °C, under which conditions they remained excitable for up to 3 days. No differences were noted in this study between channel properties in patches from fresh nerve and from nerve which had been stored for 3 days. Most of the nerves which were studied were cutaneous, either the sural nerve or the medial cutaneous nerve of the forearm, and in these cases the axons are identified as sensory in the figure legends. Axons not so identified were from mixed nerves, either ulnar, median or brachial plexus.

Individual fascicles were separated from the nerve by gripping the endoneurium with fine forceps and pulling. Surprisingly little force is required to do this, only slightly more than is required to cause the diagonal striations (p. 39 in Sunderland, 1968) to disappear, indicating straightening of the axons from their usual undulating course. We are therefore confident that the axons were not unduly stretched by this procedure. Fascicles were tied at the ends with sewing thread, pinned onto the base of a 1 ml chamber (diameter 25 mm) moulded from Sylgard 184 resin (Dow Corning, Seneffe, Belgium), and incubated in the presence of the following enzymes: first stage – 2 mg ml^{-1} collagenase (Sigma, Type XI), 0·1 mg ml^{-1} protease (Sigma, Type X), 1–2 h; second stage – 1 mg ml^{-1} protease (Sigma, Type XXIV), 30–40 min. Enzyme mixtures were made up in standard extracellular solution (see below) to which 10 mM D-glucose had been added. Incubations took place at 37 °C, with linear agitation (50 strokes min^{-1}, stroke length ~6 cm). We found it to be important for good dissociation that the fascicles were not pulled taut when pinned to the Sylgard base, so that they could move during agitation, which perhaps allowed easier access of the enzymes. After enzyme treatment, fascicles were cut into short (~2 mm) sections with fine scissors, and shaken gently to allow the nerve fibres to separate. This created a suspension of single fibres, which were transferred to 35 mm tissue culture dishes (type 25000 or 29000; Corning Glass Works, Corning, NY, USA) and allowed to settle. To improve adhesion, the dishes had already been coated with a layer of highly viscous silicone fluid (DC200/100 000 cs; Dow Corning) applied on top of a very thin layer of cured Sylgard 184.

Recording system

Patch-clamp recordings (Hamill *et al.* 1981) were made at room temperature (22–27 °C) using an Axopatch 200 amplifier (Axon Instruments, Foster City, CA, USA). Pipettes were pulled from borosilicate glass (GC150F; Clark Electromedical Instruments, Pangbourne, UK) on a Narishige PP-83 puller (Narishige Ltd, Tokyo, Japan) which had been modified by the addition of a laboratory-made constant-current circuit (±0·5 % at 13 A). They were coated with Sylgard 184 and heat-polished; bubble numbers were 2–3 (Corey & Stevens, 1983) and resistances 15–30 MΩ. The current was filtered at 10 kHz (−3 dB) using the 4-pole Bessel filter of the Axopatch, and this signal was led to a digital audiotape recorder (DTR-1202; Biologic, Claix, France) and to a 4-pole Butterworth filter (Neurolog NL125; Digitimer, Welwyn Garden City, UK) which was set to a corner frequency of 1 kHz in all the recordings presented here. The output of this filter was led to the input of an A/D converter (MC-DAS 1512; Scientific Solutions, Mentor, OH, USA), mounted in an IBM PS/2 computer. Data acquisition and control of the pulse protocols was done using pCLAMP software, version 5.6 (Axon Instruments). Data analysis was done with pCLAMP and with software written by ourselves; least-squares fits were performed using FigP software (Biosoft, Cambridge, UK). Leakage and capacity currents were compensated digitally after storage of the raw data, by subtracting currents in response to either inverted pulses, pulses that produced no channel activity, or pulses to 0 mV in symmetrical 155 mM K^+. Figures have been corrected where appropriate for a liquid junction potential of 3 mV between 155 mM KCl solution and standard extracellular solution, with the KCl solution negative (Marty & Neher, 1995).

Solutions

The standard extracellular solution contained (mM): NaCl, 154; KCl, 5·6; $CaCl_2$, 2·2; $MgCl_2$, 1·2; Hepes, 5·46; Na-Hepes (Hepes, sodium salt), 4·54 (pH 7·4 at 25 °C). The high-[K^+] extracellular solution contained: NaCl, 6·5; KCl, 155; $CaCl_2$, 2·2; $MgCl_2$, 1·2; Hepes, 5·46; Na-Hepes, 4·54 (pH 7·4 at 25 °C). The internal solution contained: KCl, 149; NaCl, 5; $CaCl_2$, 1·21; $MgCl_2$, 1·21; Hepes, 3·96; Na-Hepes, 6·04; EGTA, 3; KOH, 6 (pH 7·2 at 25 °C). The final concentration of Ca^{2+} in this solution was 10^{-7} M and of Mg^{2+} was 1·1 mM. These concentrations were calculated according to Durham (1983), with binding constants for EGTA from Harrison & Bers (1989) and Durham (1983); corrections for temperature, ionic strength, and EGTA purity were made according to Harrison & Bers (1989) and Miller & Smith (1984). External solutions contained 300 nM tetrodotoxin (TTX, Sigma) to block Na^+ currents. The K^+ channel blocker α-dendrotoxin (DTX; Latoxan, Rosans, France) was dissolved at 100 μM in distilled water, and stored at −18 °C in 10 μl aliquots; when required, the stock solution was added directly to the external recording solution, diluting that solution by up to 1 % (at 1 μM DTX). Solutions were applied

through a multi-barrel application system, described previously (Reid, 1993). Hepes and EGTA were from Sigma, and salts were from Merck.

RESULTS

Verification of patch origin

The origin of 20 outside-out patches was tested by including Lucifer Yellow CH (dilithium salt, 1 mg ml^{-1}; Sigma) in the pipette solution (Wilson & Chiu, 1990). The pattern of dye diffusion indicated that all 20 were from axonal membrane (Fig. 1*B*). We therefore consider the probability to be high that other patches were also from axonal and not Schwann cell membrane. Patches were made at nodal, paranodal and internodal sites, the maximum distance from the node being about 100 μm. The node is usually clearly distinguishable as a dark line or small bulge in the middle of the constricted axon segment (Fig. 1*A*); our use of the terms 'paranodal' and 'internodal' is based on axon diameter, with 'paranodal' referring to the constricted segment on either side of the node and the regions of the axon tapering towards it from the internode, and 'internodal' referring to the regions where the full internodal diameter has been reached.

Potassium channels activated by depolarization were present at moderately high density at all patch sites, whether nodal, paranodal or internodal. We were not able to reach firm conclusions on the density or distribution of the different channel types described below: each of them was found in patches from nodal, paranodal and internodal membrane, and no clear systematic differences were noted in patches from different sites. The classification of Jonas *et al.* (1989), described in the Introduction, is adequate for a large part of our observations, and we will use it as a starting point in the presentation of our results; the properties of the channels we have observed are summarized in Table 1. Those of our observations which are not consistent with this scheme will be evident as they arise, and will be treated further in the Discussion.

Single I channels and other types of dendrotoxin-sensitive K^+ channel

We have already published a brief description of the human I channel (Scholz *et al.* 1993). Virtually all patches contained K^+ channels of this type. Figure 2*A* shows a typical recording from an outside-out patch which contained two I channels. These channels were first activated by depolarization to around −70 mV, and fully activated at around −40 mV, reaching a maximum open probability (P_{open}) of ~0·5. The time to half-maximal activation was steeply voltage dependent in the range between −60 and −10 mV, reaching an asymptote of about 1 ms at potentials positive to +10 mV (Fig. 2*E*). The deactivation of I channels could be fitted with a single exponential, with a mean time constant of 22·5 ms at −80 mV (range 21·2–24·9 ms, $n = 3$). In their dominant gating mode (see below), their conductance in symmetrical 155 mM K^+ was about 30 pS for inward currents, and about 17 pS for outward currents; in standard extracellular solution their conductance was ohmic and around 12 pS (Fig. 2*B*).

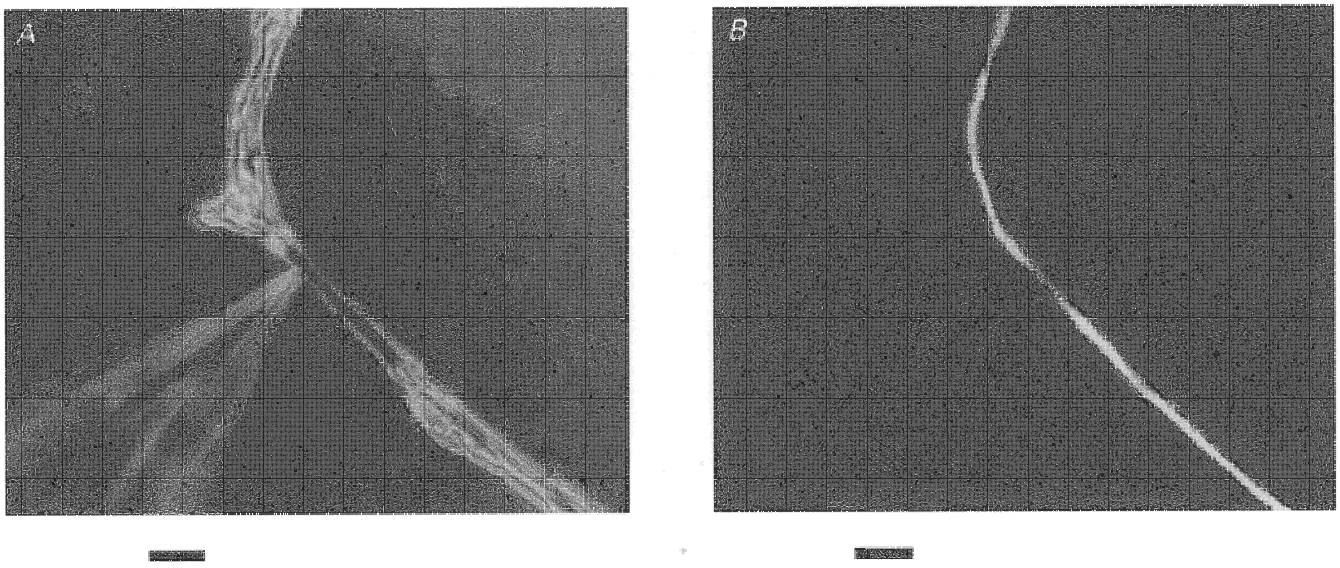

Figure 1. Human axon and Lucifer Yellow staining

A, enzymatically dissociated human myelinated axon of 12 μm diameter. The myelin had retracted by about 45 μm, uncovering the paranodal and internodal axonal membrane. The pipette contained 1 mg ml^{-1} Lucifer Yellow in standard intracellular solution. Phase contrast optics. Scale bar 20 μm for both *A* and *B*. *B*, the same axon under epifluorescence illumination after formation of an outside-out patch. Note the continuous staining of the axon on both sides of the node (the narrower region in the middle of the photo), indicating that the patch originated from axonal membrane (Wilson & Chiu, 1990).

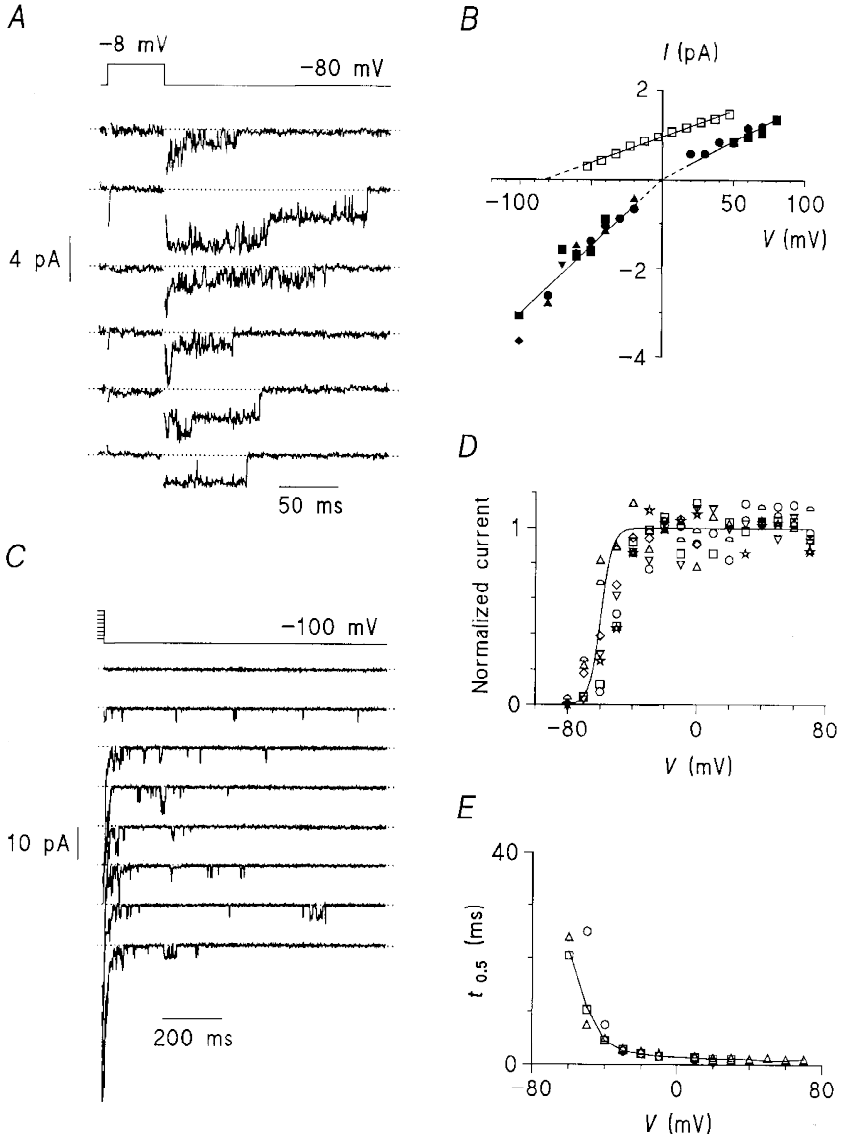

Figure 2. Properties of the I channel and the 40 pS DTX-sensitive channel

A, tail events of I channels in an outside-out patch from the internode of a human sensory axon in symmetrical 155 mM K^+. In this and other recordings, the top trace shows the command potential, and the dotted lines on each current trace indicate the closed level. Two gating modes are visible, which we have termed 'noisy' (in the second and bottom traces) and 'flickery' (in the top and third traces). These terms are explained further in the text. *B*, current–voltage relation of single I channel currents in 'noisy' mode, in two inside-out and three outside-out patches from human axons. Filled symbols show measurements in symmetrical 155 mM K^+, and open symbols measurements in standard extracellular solution; each symbol represents a different patch, except that the open and filled squares indicate currents from the same patch. Conductances were estimated by fitting linear regression lines, with those in symmetrical 155 mM K^+ constrained to pass through the origin. The conductances are: in symmetrical 155 mM K^+, inward current 30·5 pS, outward current 17·1 pS; in standard extracellular solution, outward current 11·7 pS. The extrapolated reversal potential in standard extracellular solution is about −82 mV, compared with a K^+ equilibrium potential of −83·6 mV under these conditions. *C*, re-openings of 40 pS channels at −100 mV following depolarizing pulses in an outside-out patch from the nodal region of a human sensory axon, in symmetrical 155 mM K^+. Pulses of 1 s duration were applied from a holding potential of −100 mV (only the end of the depolarizing pulse is shown). The 40 pS channels were completely silent at −100 mV and after the pulse to −80 mV (top trace), but re-opened on returning to the holding potential after larger depolarizing pulses (other traces). Pulse potentials were from −80 mV (top) to +60 mV (bottom), at 20 mV intervals. *D*, voltage dependence of activation of the I-like macroscopic K^+ current in 7 outside-out patches, in symmetrical 155 mM K^+. Each symbol represents a different patch. The smooth curve is a fit of the

Table 1. Properties of the five identified K^+ channel types in human axons

Channel name	Conductance [a] (pS)	$V_{0.5}$ [b] (mV)	k [c] (mV)	τ deactivation (ms)	τ inactivation	Block by 1 μM DTX
I (noisy mode)	30	−57	4·2	25 (at −80 mV)	7–30 s [d]	Yes
F	50	+2·8	17·9	1·4 (at −100 mV)	62 ms (at +80 mV)	No
S	10	−68	7·2	42 (at −100 mV)	No inactivation observed	No
	40	Probably fully activated at −40 mV		n.d.	Probably within 1–2 s	Yes
	25	n.d.	n.d.	n.d.	n.d.	Yes

[a] Inward current in symmetrical 155 mM K^+. [b] Half-maximal activation and [c] slope obtained from Boltzmann equation (see legend to Fig. 2*D*) in symmetrical 155 mM K^+. [d] Voltage dependent (range −40 to +80 mV). n.d., not determined (not distinguishable from I channel).

The I channel is blocked almost completely by 1 μM α-dendrotoxin (DTX; Scholz *et al.* 1993). Some patches contained other types of DTX-sensitive K^+ channel, with conductances for inward current of about 40 pS and about 25 pS in symmetrical 155 mM K^+. The 40 pS channel showed brief re-openings on returning to the holding potential after depolarizing pulses (Fig. 2*C*), a feature never observed in the I channel. The re-openings were most frequent immediately after the end of the depolarizing pulse, and declined over a period of some hundreds of milliseconds thereafter. Their presence depended on channel activity during the depolarizing pulse: pulses which elicited no channel activity were not followed by re-openings, and their frequency increased with the potential of the depolarizing pulse between −70 and −40 mV. These characteristics of the re-openings are consistent with recovery from N-type inactivation (see Discussion).

Two modes of I channel gating

In several patches, the I channel displayed two different conductance levels in tail events, which are visible in Fig. 2*A*. The most frequent type, visible in the second and bottom traces in this figure, had a 'noisy' appearance, characterized by long openings and very brief, incompletely resolved closings, and had a conductance of about 30 pS for inward currents in symmetrical 155 mM K^+. The other type, seen in the top and third traces, showed bursts of shorter openings, with longer, well-resolved closings, giving these events a 'flickery' appearance. The conductance of these openings was about 22 pS. About 10 % of tail events in this patch were in 'flickery' mode, and about 90 % in 'noisy' mode.

At first sight it appeared that this patch contained channels of two types: I channels, producing the 'noisy' events, and channels of a different type, responsible for the 'flickery' events. However, if this were the case, the patch would have had to contain at least four channels, because some tails contained two 'noisy' channels and others two 'flickery' channels (see Fig. 2*A*, top and second traces). We estimated the channel number using binomial statistics (Colquhoun & Hawkes, 1983): in tail currents following 284 depolarizing pulses to −8 mV, over a 20 min period, about half contained a maximum of one or two simultaneous openings, with none containing more than two. This is consistent with binomial statistics for a patch containing two channels, but if the patch had contained four independent channels, we should have observed three or four simultaneous openings in 14 % (40/284) of the tail currents. We therefore conclude that the patch contained only two channels, which alternated between the 'flickery' and 'noisy' modes of gating. Switching between these two gating modes, with no intervening closure that could be resolved, was occasionally observed directly during single bursts of I channel openings in other patches (not shown).

When the distribution of times until the last closing of the channels during tail currents was plotted for 'noisy' and 'flickery' tail events, the 'noisy' mode of gating produced a distribution with a single time constant of 24·9 ms at −80 mV (Fig. 3*B*, top), close to that of the averaged I channel tail current (see above). The 'flickery' mode of gating produced an additional slower component, with a time constant of 102 ms (Fig. 3*B*, bottom), similar to the

Boltzmann function $f(V) = 1/(1 + \exp((V_{0.5} - V)/k))$ to the voltage dependence of the I channel (Scholz *et al.* 1993) with $V_{0.5} = -57{\cdot}3$ mV and $k = 4{\cdot}2$ mV. Fits of the Boltzmann function to the macroscopic currents have been omitted for clarity; the values obtained were: $V_{0.5} = -55{\cdot}3 \pm 6{\cdot}8$ mV; $k = 5{\cdot}9 \pm 1{\cdot}4$ mV (mean ± S.D., $n = 7$). *E*, continuous line: voltage dependence of the time to half-maximal activation ($t_{0.5}$) of the I channel in symmetrical 155 mM K^+, in an inside-out patch from the paranode of a human axon, measured at 10 mV intervals from −60 to +70 mV (symbols have been omitted for clarity). Open symbols: time to half-maximal activation of the I-like macroscopic K^+ current component in 3 outside-out patches. The same symbols have been used for each patch in *D* and *E*.

deactivation time constant of the slow component of macroscopic K^+ current in some patches (see below).

The 'flickery' mode activated at more negative potentials than the 'noisy' mode: in some patches, sporadic openings in the 'flickery' mode were already apparent at −80 mV, and constituted the whole of the channel activity at this potential. The activation of 'flickery' activity at −80 mV, from a holding potential of −120 mV, was slow and could be described by a single exponential, with a time constant of 50 ms (not shown).

Macroscopic currents with I-like kinetics

In large tail currents (50–250 pA) recorded in symmetrical 155 mM K^+, the deactivation process could be described by the sum of two or three exponential functions. In all of 30 large patches, the largest component of macroscopic K^+ current (about 50–75% of the current in most patches, and virtually all of the current in some patches) had a voltage dependence and time course similar to that of the I channel in its 'noisy' gating mode (see above). At a holding potential of −100 mV, the mean time constant was 12·1 ms (range 7·6–15·5 ms, $n = 5$), and at −80 mV, it was 17·5 ms (range 10·7–29·2 ms, $n = 3$). In all of seven patches, this current component was blocked completely by 1 μM DTX (Fig. 3*A*).

The voltage dependence of activation of this component is shown in Fig. 2*D*, and the time course of its activation in Fig. 2*E*. In both of these respects, as well as its deactivation kinetics and its DTX sensitivity, its behaviour is accounted for satisfactorily by the properties of single I channels in the 'noisy' gating mode.

Inactivation of the I channel and of the macroscopic I-like current

In patches with large K^+ currents, the inactivation process at −40 mV had both fast and slow components; the slower component could be fitted with a single exponential, with a mean time constant of 13·1 s (range 7·2–20·7 s, $n = 3$; Fig. 4*A*), while the faster component had a time constant of about 2 s. Both were blocked by 1 μM DTX. The slower of the two processes can be accounted for by the inactivation of the I channel: it could be followed at potentials between −60 and +60 mV in one patch, where the currents were large enough to allow measurement of the time constant,

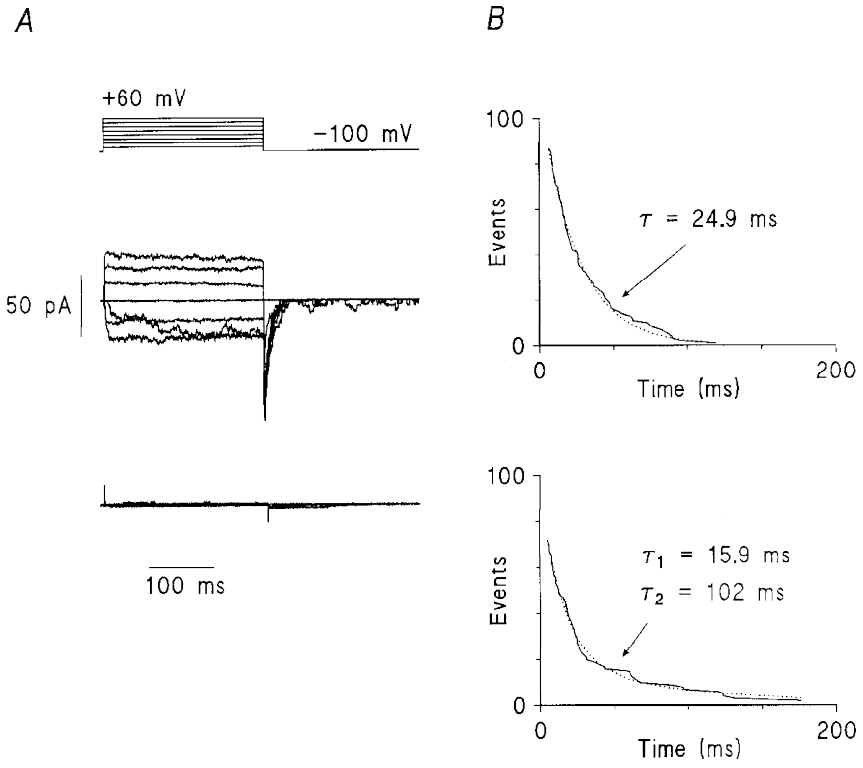

Figure 3. Block of the I channel current by DTX and kinetics of its two gating modes

A, block of the I-like macroscopic current by α-dendrotoxin (DTX): K^+ currents in an outside-out patch from the paranode of a human sensory axon, in symmetrical 155 mM K^+, before (above) and after (below) the application of 1 μM DTX. Almost all of the current was blocked by DTX. Re-openings of 40 pS channels (see text and Fig. 2*C*) are visible after the tail currents, and these were also blocked by DTX. A few S channels (see text and Fig. 5) remained after DTX block. *B*, cumulative distributions of times until the last closing of the channels during I channel tail events in the patch shown in Fig. 2*A*. Top: distribution of 'noisy' tail events ($n = 88$); bottom: distribution of 'flickery' tail events ($n = 73$). Dotted lines show fits of one ('noisy') or two ('flickery') exponential functions, with the time constants (τ) shown.

but small enough for single I channels to be visible during much of the inactivation process (Fig. 4*B*, bottom trace). Inactivation became slower at more positive potentials (Fig. 4*C*), and it was incomplete at potentials positive to +30 mV (Fig. 4*B*, top two current traces): at these potentials, I channels remained active throughout pulses of several minutes duration. A related observation is that complete inactivation of the I channel at −40 mV could be overcome by strong depolarizing pulses (Fig. 4*D*). Strong depolarizing pulses could also relieve DTX block: in the presence of 1 μM DTX, single I channel activity was visible during pulses positive to +30 mV, although the block was complete at more negative potentials (not shown). The voltage dependence of the current escaping from DTX block was similar to that escaping from inactivation. The implications of these observations for the mechanism of inactivation are considered in the Discussion.

The voltage dependence of steady-state inactivation of the macroscopic I-like current was followed in one patch in which the currents were dominated by this component. Holding potentials between −100 and −40 mV were maintained for at least 3 min, and then 250 ms depolarizing pulses were applied at 2 s intervals to potentials between the holding potential and +60 mV. Steady-state inactivation at a given holding potential was estimated by measuring the current amplitude during each depolarizing pulse (at 25 ms), and expressing this as a fraction of the current amplitude during the same depolarizing pulse from a holding potential of −100 mV; this fraction was then averaged across all the depolarizing pulses at each holding potential. The voltage dependence of inactivation is shown in Fig. 4*E*. The maximum of the fitted Boltzmann function is around 5% greater than the current at −100 mV, implying that only a small fraction of the K^+ current is inactivated at −100 mV. The fit is subject to some uncertainty because the patches often became unstable at potentials negative to −100 mV, making measurements in this region difficult. About half of it is inactivated at −80 mV. To eliminate the possibility that the small rapidly inactivating current in this patch affected the measurement, we estimated the voltage dependence of inactivation from currents near the beginning (at 25 ms) and at the end of the 250 ms depolarizing pulses. The measurements were identical, implying either that the fast-inactivating component had a negligible effect on the measurement, or that the voltage dependence of inactivation of the two components is similar; in either case, the measurements are a good estimate of the steady-state voltage dependence of I channel inactivation.

Single S channels

In six of seven patches, block of the I channel current with 1 μM DTX (Fig. 3*A*) revealed identifiable single channels of other types. In five of these patches, we observed a channel with small conductance (Fig. 5*A*), which became active at around −80 mV, and deactivated more slowly at −100 mV than the I channel. It appears to be the same as the S channel in *Xenopus* and rat axons (Jonas *et al.* 1989; Safronov *et al.* 1993), and will also be called the S channel in this study.

The amplitudes of single S channel currents are shown in Fig. 5*B*. In symmetrical 155 mM K^+, the conductance of this channel type for inward current was usually around 10 pS. Two S channels in one patch had a distinctly smaller current than the rest, and these currents have been fitted separately in this figure to reveal a conductance of ∼7 pS. We could not measure the conductance of the S channel for outward current because its activation was rapid at positive potentials, and it usually remained open once activated, without the brief closings during depolarizing pulses which we observed in I channels.

In the patch shown in Fig. 5*A*, the number of S channels was estimated to be three using binomial statistics. The voltage dependence of their open probability is shown in Fig. 5*C*. Like I channels, the maximum open probability of S channels was substantially less than 1: in the patch shown in Fig. 5*A* it was 0·62. Their activation was steeply voltage dependent over the range of potentials from −80 to −50 mV, slightly more negative than the range of potentials over which the I channel is activated. The deactivation of the S channels in this patch was fitted well by a single exponential with a time constant of 41·7 ms at −100 mV.

Macroscopic currents with slow kinetics

In almost all patches with large K^+ currents, a fraction of the tail current (up to 25%) deactivated more slowly than the component associated with the I channel. In some cases, we could account for this component by the properties of single S channels. In other cases, as described below, its origin is different.

In four of five patches, the time constant of deactivation was around 40 ms at −100 mV, similar to that of the S channel. The voltage dependence of activation of the slow component in these four patches, measured as described above for the intermediate component, is shown in Fig. 5*C*. In two of these four patches, the voltage dependence of activation was indistinguishable from that of the S channel (Fig. 5*Ca*), while in the other two, it was much less steep (Fig. 5*Cb*). In only two of these four patches, therefore, can the slow component of macroscopic K^+ current be accounted for by the properties of single S channels. We did not observe any single channels whose voltage dependence could account for the macroscopic currents in Fig. 5*Cb*.

In the fifth of these patches, deactivation was much slower, with a time constant of about 90 ms at −100 mV and a little over 100 ms at −80 mV. In addition, in this patch, no S channels were visible in tail currents; instead, the channel activity resembled the I channel in its 'flickery' mode (see above). The deactivation time constant was also consistent with 'flickery' gating of I channels, and the voltage dependence of activation of the slow K^+ current component in this patch (not shown) was indistinguishable from that of the I channel. We therefore conclude that the slow component

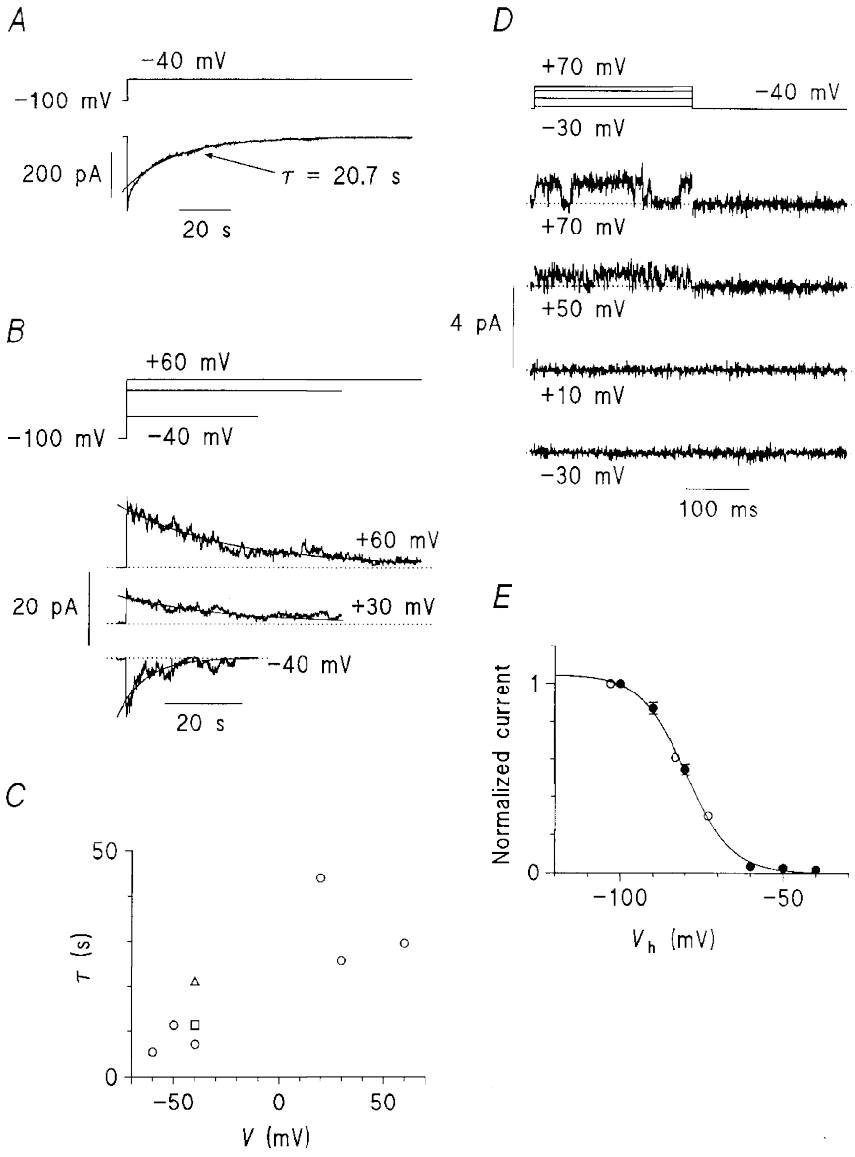

Figure 4. Inactivation of the I channel current

A, K^+ current inactivation at −40 mV in an outside-out patch from the paranode of a human sensory axon, in symmetrical 155 mM K^+. The slow phase of inactivation is fitted by a single exponential (smooth curve) with a time constant (τ) of 20·7 s. *B*, K^+ current inactivation at several potentials, in an outside-out patch from the internode of a human sensory axon, in symmetrical 155 mM K^+. The patch contained about 20–25 I channels. The smooth curves are single exponential functions fitted to the decay of the current; time constants were: −40 mV, 7·2 s; +30 mV, 25·8 s; +60 mV, 29·6 s. *C*, time constants of single exponential fits to slow inactivation in the patch shown in *B* (circles). Single measurements at −40 mV in two other outside-out patches are also shown (other symbols). *D*, after complete inactivation of I channels at a holding potential of −40 mV, strong depolarizing pulses elicited occasional I channel activity ('knockout'). Outside-out patch from the internode of a human sensory axon, containing about 40 I channels, in symmetrical 155 mM K^+. *E*, voltage dependence of inactivation of the K^+ current in the same patch as in *D*. From holding potentials (V_h) between −100 and −40 mV, 250 ms depolarizing pulses were applied to potentials between the holding potential and +60 mV. The currents elicited at each holding potential were averaged across all the depolarizing pulses and normalized, with the currents from a holding potential of −100 mV represented by a value of 1. Current amplitudes were measured 25 ms into the pulse in standard extracellular solution (○) and symmetrical 155 mM K^+ (●). The smooth curves are fits of the Boltzmann function $f(V) = I_{max}/(1 + \exp((V - V_{0.5})/k))$ with the values: $V_{0.5} = -79{\cdot}8$ mV, $k = 6{\cdot}9$ mV, $I_{max} = 1{\cdot}05$.

in this patch was satisfactorily accounted for by the I channel in its 'flickery' mode.

To summarize, the slow component in patches with large K^+ currents can only partially be accounted for by the S channel; part of it is produced by the I channel in its 'flickery' gating mode, and the remainder does not correspond to any identified type of single channel.

Single F channels

In two of seven patches, application of 1 μM DTX revealed single channels with a large conductance, activating at more positive potentials than the I channel (Fig. 6*A*). They deactivated very rapidly ($\tau = 1{\cdot}4$ ms at -100 mV) and inactivated over a period of a few hundred milliseconds. They showed occasional re-openings on returning to the holding potential after depolarizing pulses. This channel type appears to be the F channel described in *Xenopus* and rat (Jonas *et al.* 1989; Safronov *et al.* 1993), and will also be called the F channel here. F channels were rarely encountered in human axons: in only two of six patches where 1 μM DTX exposed single channels were they F channels, and we never saw them in single-channel patches without DTX. This is in apparent contrast to rat axons (see Discussion).

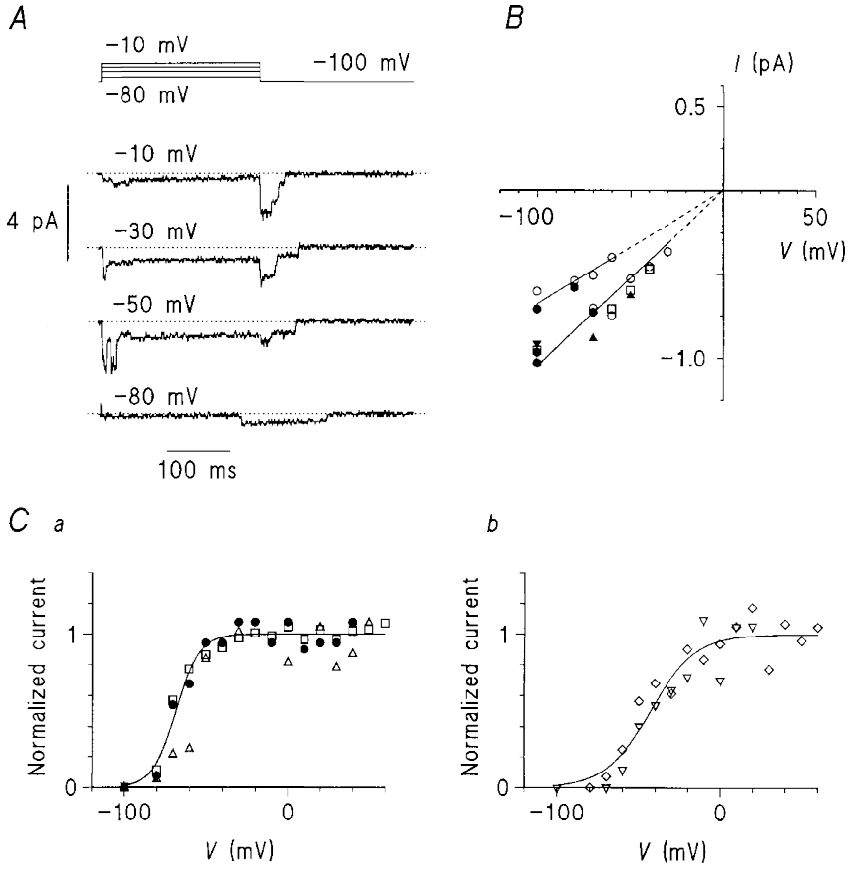

Figure 5. Properties of the S channel and the slow macroscopic K^+ current

A, currents through S channels in an outside-out patch from the paranode of a human sensory axon, in symmetrical 155 mM $K^+ + 1$ μM α-dendrotoxin (DTX). *B*, current amplitudes through single S channels in 4 outside-out patches in symmetrical 155 mM K^+. Measurements made in the presence of 1 μM DTX are shown as open symbols, and without DTX as filled symbols; the circles indicate measurements from the patch shown in *A*. The straight lines are linear regression lines constrained to pass through the origin, and indicate conductances of 10·5 and 6·8 pS. *Ca*, normalized open probability of the S channels in the patch shown in *A* (filled circles), measured after 250 ms pulses to potentials between -80 and $+40$ mV, from a holding potential of -100 mV. The smooth curve is a fit of the Boltzmann function (see Fig. 2) to these points with the following values: $V_{0{\cdot}5} = -68{\cdot}1$ mV; $k = 7{\cdot}2$ mV. The open symbols show the voltage dependence of activation of the slow component of macroscopic K^+ current in two outside-out patches. Values obtained from fits of the Boltzmann function in these patches (fitted curves omitted for clarity) were: $V_{0{\cdot}5} = -69{\cdot}5$ and $-57{\cdot}2$ mV, $k = 7{\cdot}5$ and 4·5 mV. *Cb*, voltage dependence of activation of the slow component of macroscopic K^+ current in two further outside-out patches where the voltage dependence of activation of the slow component was much less steep than that shown in *Ca*. A Boltzmann function (Fig. 2) is fitted to the points (smooth curve); the values obtained from the fit were: $V_{0{\cdot}5} = -42{\cdot}9$ mV, $k = 13{\cdot}8$ mV.

The conductance of the F channel was about 50 pS for inward current and about 30 pS for outward current in symmetrical 155 mM K^+ (Fig. 6*B*). The voltage dependence of activation could be estimated in only a single patch, which contained at least three F channels (the data were not sufficient to allow us to estimate the channel number using binomial statistics). The voltage dependence of activation is shown in Fig. 6*C*; the potential for half-maximal activation is close to 0 mV, more than 40 mV positive to that of the I channel, and the slope is substantially less steep. The maximum P_{open}, like that of the I and S channels, is less than 1: the maximum of a Boltzmann function fitted to the number of open channels corresponded to 2·4 open channels at potentials positive to +40 mV, implying a maximum P_{open} of not more than 0·8. The F channel activated at a similar rate to the I channel, but at potentials about 20 mV more positive (Fig. 6*D*).

F channel inactivation was recorded at +80 mV (Fig. 7*A*). The time course of inactivation at this potential can be fitted with a single exponential with a time constant of 62 ms, but inactivation was not complete: although the 250 ms pulses were sufficiently long for this process to have reached a steady state, some openings of single F channels remained visible throughout the depolarizing pulses.

Macroscopic currents with fast deactivation and fast inactivation

Some patches with large K^+ currents displayed two features reminiscent of F channels: a fast component of deactivation, and a fast phase of inactivation. We will deal with deactivation first.

After short depolarizing pulses, a fast component of deactivation with a time constant of 1–2 ms was revealed

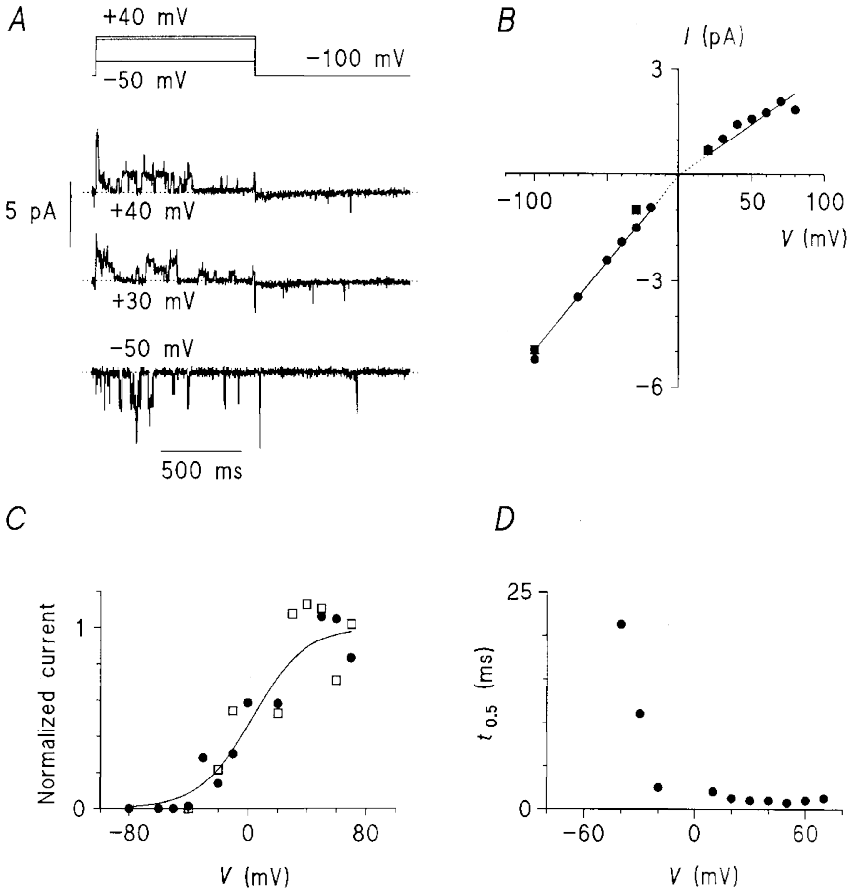

Figure 6. Properties of the F channel and the fast macroscopic K^+ current

A, currents through F channels in an outside-out patch from the nodal region of a human sensory axon in symmetrical 155 mM K^+ + 1 μM DTX. *B*, the amplitudes of currents through single F channels in two outside-out patches, recorded in symmetrical 155 mM K^+ + 1 μM DTX. Currents in one patch (circles) are shown in *A*; the other patch was from the paranode of a human sensory axon. Linear regression lines constrained to pass through the origin reveal conductances of 49·7 pS for inward current, and 28·9 pS for outward current. *C*, ● represents voltage dependence of activation of F channels in the patch shown in *A*; the smooth curve is a fit of the Boltzmann function (see Fig. 2) to these points, with the values $V_{0.5} = +2{\cdot}8$ mV and $k = 17{\cdot}9$ mV. □ represents the voltage dependence of activation of the fast-deactivating component of macroscopic K^+ current in an outside-out patch from the paranode of a human axon, in symmetrical 155 mM K^+; a fit of the Boltzmann function (see Fig. 2) to these points (omitted for clarity) gave the values $V_{0.5} = -4{\cdot}0$ mV and $k = 15{\cdot}1$ mV. *D*, voltage dependence of the time to half-maximal activation ($t_{0.5}$) of F channels in the patch shown in *A*.

by fitting sums of exponential functions to macroscopic tail currents. Its amplitude was usually too small to allow its characteristics to be measured. However, one patch had a fast component making up almost half of the total current, and we analysed this in detail. The fast component was present after pulses to potentials between −40 and +70 mV. In order to test whether its voltage dependence of activation was consistent with that of the F channel, we subtracted the tail currents after pulses to −40 mV (this potential is sufficient to fully activate the I and S channels, but only minimally activates the F channel) from those after pulses to more positive potentials. The current resulting from this subtraction had a time constant of deactivation of 2·4 ms at −80 mV (compared with 1·4 ms for the F channel; see above). Its amplitude was measured by fitting a 2·4 ms exponential component to the subtracted tail currents, and the resulting voltage dependence of activation, shown in Fig. 6*C*, was indistinguishable from that of the F channel. We therefore conclude that the fast-deactivating K^+ current in this patch is adequately accounted for by the F channel.

A more noticeable feature in macroscopic currents was the fast component of inactivation. A fast-inactivating component of the K^+ current was visible in about half of all large patches, and in three patches it was large enough to measure its amplitude and time course. Fits of a single exponential function to the fast inactivation process in these patches produced a time constant which was steeply voltage dependent, from around 500 ms at −40 mV to around 100 ms at +60 mV. However, the quality of the fit was poor at potentials positive to +10 mV, and a better fit was obtained with two time constants (Fig. 7*B*). The faster of

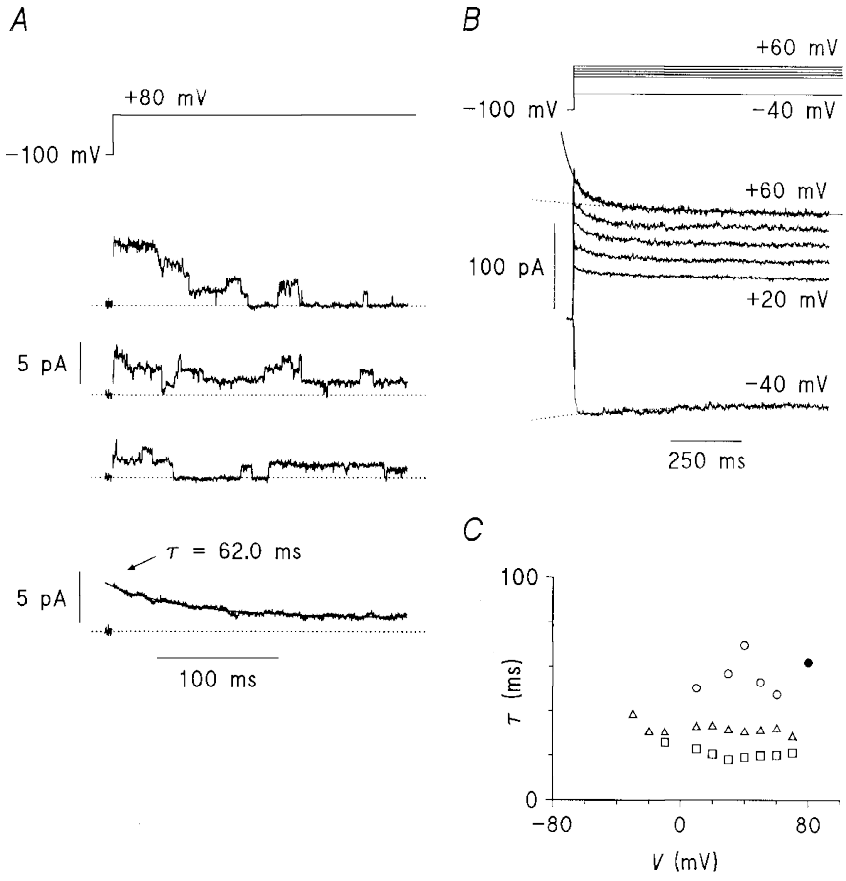

Figure 7. Inactivation of the F channel and of the fast macroscopic K^+ current

A, top three current traces: F channel currents in the patch shown in Fig. 6*A*, in symmetrical 155 mM K^+, during 250 ms depolarizing pulses to +80 mV; bottom trace: averaged F channel currents from 21 pulses to +80 mV. The smooth curve shows a single exponential function fitted to the averaged current, with time constant $\tau = 62$ ms. *B*, K^+ currents in an outside-out patch from the paranode of a human sensory axon, in symmetrical 155 mM K^+, during 1 s pulses to −40, +20, +30, +40, +50 and +60 mV. The inactivation of the current in response to the −40 mV pulse is fitted with a single exponential function (dotted line) with a time constant of 406 ms. The inactivation at +60 mV is fitted with the sum of two exponential functions (smooth curve), with the slower time constant fixed at 500 ms (dotted line); the faster time constant was 47·5 ms. *C*, time constants (τ) of the faster of the two inactivation processes shown in *B*, plotted against voltage. The open circles are measured from the currents shown in *B*, and the other open symbols are from two other outside-out patches, measured in the same way. The time constant of F channel inactivation at +80 mV (from *A*) is shown for comparison (●).

these two time constants is similar to that obtained from recordings of single F channels. The slower component is present at potentials as negative as −40 mV (see also Fig. 4*A*), at which few F channels are active (see Fig. 6*C*). Its amplitude did not increase at potentials positive to −40 mV, suggesting that it is due to channels which are already fully active at this potential and not to the F channel (see Discussion). It is about 10 times faster than the I channel inactivation process described above.

These observations suggest that there are two components of fast inactivation, one about an order of magnitude faster than the other, and that the apparent voltage dependence of the rate of inactivation at potentials positive to +10 mV (becoming faster at more positive potentials) is actually due to the voltage dependence of the amplitude of the faster component (which becomes larger at more positive potentials). Accordingly, the currents in these three patches at −40 mV were fitted with a single exponential function, producing a time constant of around 0·5–1 s, and this time constant was fixed when subsequently fitting the sum of two exponential functions to currents at more positive potentials (Fig. 7*B*). The resulting fits were much improved over those with only a single exponential, and the faster time constant was insensitive to changing the slower one between 0·5 and 2 s. The faster time constant of inactivation in four patches is plotted against voltage in Fig. 7*C*. It is close to that measured for the F channel (see above), and does not appear to be voltage dependent.

We therefore conclude that the fast components of macroscopic K^+ current inactivation result from two channel types. The faster component of inactivation, with a time constant around 50 ms, can be accounted for by the F channel. The slower, with a time constant of 0·5–2 s, is associated with a conductance which is already fully activated at −40 mV and is blocked by 1 μM DTX. Its origin is considered further in the Discussion.

DISCUSSION

Similarities and differences between human and rat axonal potassium channels

Our results can be compared directly in most cases with measurements in rat axons (Safronov *et al.* 1993), and in some cases with those in *Xenopus* axons (Schwarz & Vogel, 1971; Koh & Vogel, 1996) where the rat data are unavailable. Figure 8 shows the voltage dependence of activation of the human I-like macroscopic current and the human S and F channels, compared with the corresponding measurements in rat axons reported by Safronov *et al.* (1993). Measurements in the two species are closely similar; the difference is no greater than the variation observed within one species, in single *Xenopus* I channels (Jonas *et al.* 1989; Koh & Vogel, 1996). The time to half-maximal activation of the human I channel is comparable to that in *Xenopus* (Koh & Vogel, 1996), when allowance is made for the difference in temperature, assuming a Q_{10} (temperature coefficient over a 10 °C temperature range) of about 3. The time constants of deactivation of the I and F channels are almost identical to the corresponding measurements in the rat, but the human S channel deactivates about three times faster than that in the rat; a similar species difference is evident in the slow macroscopic K^+ current in voltage-clamped nodes (Röper & Schwarz, 1989; Schwarz *et al.* 1995). The I channel in excised patches deactivates much more slowly than the current in intact nodes which it probably underlies (Schwarz *et al.* 1995); this discrepancy has already been commented on in rat and *Xenopus* axons (Jonas *et al.* 1989; Safronov *et al.* 1993), and the cause remains to be explained. Inactivation of the human I channel appears to be somewhat slower than that in the rat at +40 mV, and that of the human F channel more rapid. The voltage dependence of I channel inactivation is similar to that of the slow component of K^+ current inactivation in *Xenopus* (Schwarz & Vogel, 1971) and, as in that study, inactivation of the human I channel becomes slower and remains incomplete at more positive potentials.

One of the aims of this study was to try to explain the differences in electrotonus measured *in vivo* by Bostock & Baker (1988). In that study, electrotonus in rat axons was made more similar to that in human axons by application of low concentrations of 4-aminopyridine (4-AP) and tetraethylammonium, which block fast and slow K^+ conductances, respectively (Baker *et al.* 1987). This suggests that in rat axons, more K^+ channels are active near the resting potential than in human axons, which could be the result of a higher density, or a different voltage dependence of activation. Patch-clamp studies give us no reliable information about channel density; as far as the voltage dependence is concerned, we found no evidence of a species difference between rat and human axons for any of the three major K^+ channel types. None of the other minor species differences in K^+ channel properties mentioned above is capable of explaining the electrophysiological differences observed *in vivo* between rat and human axons by Bostock & Baker (1988).

The possibility remains, however, that the quantitative species differences we have observed could have physiological implications. The faster rate of deactivation of the human S channel than that of the rat would produce different behaviour during trains of action potentials at moderate frequencies, within the range commonly encountered in motor fibres and large afferents: assuming a Q_{10} of about 3, at a frequency of 20 Hz *in vivo* the human S channel would be expected to deactivate completely between impulses, while the rat S channel would remain substantially open, lowering the safety factor for conduction of sustained trains of impulses. The recently described frequency-dependent conduction block in single peripheral nerve fibres of human subjects (Inglis *et al.* 1998) could also be due to the rate of S channel deactivation. Here, conduction block was observed

at frequencies of 20 Hz and above, and conduction was restored at lower frequencies. At frequencies above 20 Hz, we would expect the S channel to deactivate incompletely between impulses, leading to a raised threshold for the generation of subsequent action potentials. We suggest that conduction failure during naturally evoked activity might be explained on the basis of the K^+ channels described in this study.

There is circumstantial evidence that F channels are less frequent in human than in rat axons: block of I channels by DTX in rat axons leaves a relatively homogeneous population of F channels (Safronov *et al.* 1993), whereas in human axons we observed S channels much more commonly than F channels in 1 μM DTX (see Results). Similarly, patches from rat axons are occasionally dominated by an F channel component (Schneider *et al.* 1993), whereas we found that all of 30 large patches from human axons were dominated by the I channel component. However, since F channels are expected to be closed near the resting potential, this difference is not likely to be responsible for the differences in electrotonus.

Which types of potassium channel are present in human axons?

While our results are in accordance with the idea that the three components of macroscopic K^+ current first identified by Dubois (1981) are largely contributed by the three types of K^+ channel described by Jonas *et al.* (1989) and Safronov *et al.* (1993), some of our observations indicate that the picture is more complex.

A single channel type can produce behaviour associated with more than one macroscopic current component. The I channel has two modes of gating, named here 'noisy' and 'flickery'; two different gating modes have also been mentioned in the *Xenopus* I channel (Koh & Vogel, 1996). The 'noisy' mode is the more frequent, and underlies the largest component of macroscopic K^+ current (see Results). However, deactivation in the 'flickery' mode has an additional, slower time constant, and we have shown that the 'flickery' mode of the I channel can account for part of the slow macroscopic current. It is interesting in this connection that Dubois (1981) observed a bi-exponential time course for the deactivation of the I_{Kf1} component of macroscopic K^+ current in intact frog axons, with one time constant about four times longer than the other. This behaviour is expected to produce a DTX-sensitive I_{Ks}-like current with a predominantly paranodal and internodal location (Röper & Schwarz, 1989), which would explain some of the effects of DTX on the slow process of accommodation (Poulter *et al.* 1989).

The slow macroscopic current is therefore contributed by several channel types: we have shown that in some patches, the slow component of macroscopic current can be accounted for adequately by the S channel, and in others, as discussed above, by the 'flickery' mode of the I channel; however, in other patches, the slow K^+ current behaves differently from either of these two channel types. The voltage dependence of activation of the I and S channels is quite different from that of I_{Ks} in intact nodes: the I and S channels activate steeply at potentials between −70 and

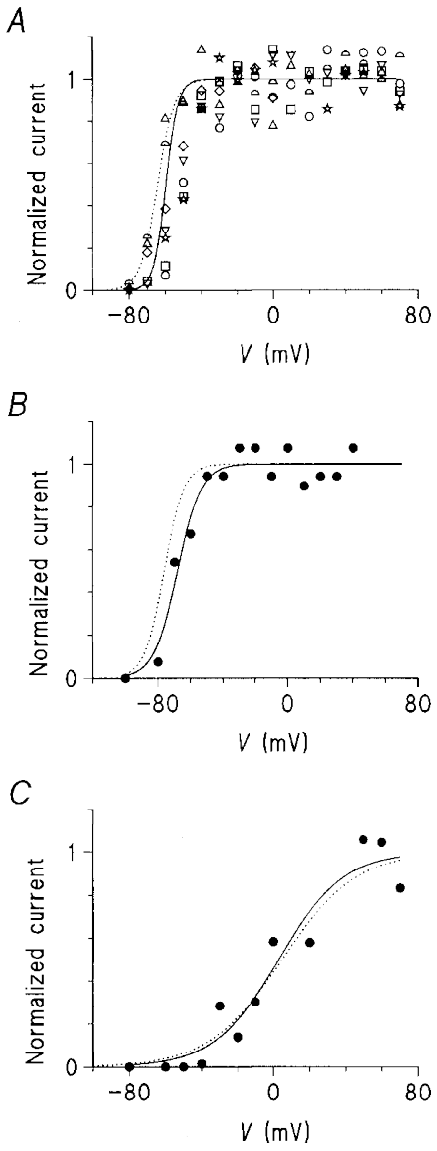

Figure 8. Comparison of the properties of the I, S and F channels in human and rat axons

A, voltage dependence of activation of the macroscopic I-like current (symbols) and the I channel (continuous line) in human axons (data from Fig. 2*D*), and of the macroscopic I-like current in rat axons (dotted line; Boltzmann function with $V_{0.5} = -64{\cdot}2$ mV and $k = 4{\cdot}8$ mV, from Safronov *et al.* 1993). *B*, voltage dependence of activation of the S channel in a human axon (symbols and continuous line; data from Fig. 5*Ca*) and in a rat axon (dotted line; Boltzmann function with $V_{0.5} = -76{\cdot}3$ mV and $k = 6{\cdot}0$ mV, from Safronov *et al.* 1993). *C*, voltage dependence of activation of the F channel in a human axon (symbols and continuous line; data from Fig. 6*C*) and in a rat axon (dotted line; Boltzmann function with $V_{0.5} = +4{\cdot}6$ mV and $k = 20{\cdot}4$ mV, from Safronov *et al.* 1993).

−40 mV, while the nodal I_{Ks} activates much less steeply, over a range from −100 to 0 mV (Schwarz *et al.* 1995). The same discrepancy is evident in the rat (Röper & Schwarz, 1989; Safronov *et al.* 1993). In two patches in this study (Fig. 5*Cb*), the voltage dependence of the slow macroscopic current was more similar to that of the macroscopic I_{Ks} current in the node of Ranvier than to that of the S channel. It is possible that the slow macroscopic current is made up of the S channel, the I channel in its 'flickery' mode, and another channel type, as yet unidentified; another possibility is that a cytoplasmic component, missing in excised patches, modifies the voltage dependence of the S channel to make it more similar to I_{Ks} in intact nodes.

The DTX-sensitive channel family and K^+ channel inactivation

Along with the rat I channel, Safronov *et al.* (1993) described a channel with a conductance of 40 pS, which they suggested was a subtype of the I channel. The I channel and the 40 pS channel are also present in human axons, as well as an apparently I-like channel with a conductance of about 25 pS, and all three are blocked by 1 μM DTX. This finding is in accord with immunocytochemical evidence in central myelinated axons: both Kv1.1 and Kv1.2 α-subunits are present, and they form heteromultimeric channels *in vivo* (Wang *et al.* 1993), suggesting that (if the situation in peripheral nerve is similar) we ought to find at least three distinct but related DTX-sensitive K^+ channels in axons. More recent studies in rat dorsal root ganglion cells (Gold *et al.* 1996; Safronov *et al.* 1996) show a similar variety of delayed rectifier K^+ channels. However, the observation that most of the K^+ current in human axons is blocked by 1 μM DTX (Fig. 3*A*) implies that a limited set of α-subunits may contribute the major part of the K^+ current, since only three types of α-subunit are known to be DTX sensitive (Kv1.1, Kv1.2 and Kv1.6; Robertson, 1997).

The observation that the 40 pS channel re-opens on returning to the holding potential after a depolarizing pulse (Fig. 2*C*) suggests that it may inactivate by an N-type ('ball-and-chain') mechanism. N-type inactivation has features in common with intracellular open-channel block (Demo & Yellen, 1991), including the presence of re-openings during recovery from inactivation: the 'ball' is considered to block the channel in the open state, and must unbind from its site before the channel can close. The time course of the re-openings we observed in the 40 pS channel, and their dependence on previous channel activity, are exactly what would be predicted from a mechanism like that described by Demo & Yellen (1991) in the *Shaker* H4 channel. If this is the case, it would imply that the inactivation of the 40 pS channel is rapid, because the 1 s pulses preceding the tail currents in Fig. 2*C* must already have induced substantial inactivation; this makes the 40 pS channel a likely candidate for the channel underlying the 0·5–2 s component of inactivation. This suggestion is supported by recent work in rat axons, showing that the 0·5–2 s component of inactivation is contributed by a channel which is distinct from the I channel and which has two mechanisms of inactivation, one fast and one slow (G. Reid, V. Ristoiu, A. Babeş & T. Gliga, unpublished).

In contrast, the I channel in human axons does not appear to inactivate by an N-type mechanism; since the molecular mechanisms of slow inactivation have recently been studied intensively in cloned K^+ channels, it was of interest to us to compare the features of slow inactivation in this native K^+ channel with those described for cloned channels. Two observations we made in this study – the slower and incomplete inactivation in patches held at positive potentials, and the 'knockout' of inactivation by brief pulses to positive potentials – suggest that outward K^+ current may antagonize I channel inactivation, as has been reported for C-type inactivation (Baukrowitz & Yellen, 1995). However, the voltage dependence of the rate of C-type inactivation in a Kv1.4 channel (Rasmusson *et al.* 1995) is clearly different from that in the I channel reported here. It is therefore not safe to suppose that the slow inactivation of the I channel is C-type.

In summary, we have shown that the three major types of voltage-gated K^+ channel identified in human axons are quantitatively very similar to the corresponding channel types in rat axons, apart from minor differences in their kinetics. In addition, there are two other types of DTX-sensitive channel with some similarities to and some differences from the I channel, and there may be one more K^+ channel with slow kinetics. It seems puzzling that the axon expresses several channel types whose macroscopic behaviour in excised patches is so difficult to distinguish. One obvious possibility is that their behaviour is not always similar in the intact axon, because they are modulated in different ways (Chung & Kaczmarek, 1995). Our results and those from previous patch-clamp studies in axons suggest that the I channel (and perhaps the S channel too) requires some cytoplasmic factor, missing in excised patches, for its normal function. In recent years, the study of ion channel modulation has revealed a fascinating complexity, yet we know little of how these processes operate in axons, and this area appears ripe for investigation.

One situation in which small molecular differences between apparently similar K^+ channels may become practically important is when it becomes desirable to block them, for instance in the symptomatic treatment of multiple sclerosis. Some success in this direction has been achieved with 4-AP (Davis *et al.* 1990; Schwid *et al.* 1997), but its side effects can be distressing because it blocks a variety of K^+ channel types. A more targeted approach, directed towards one subtype of axonal ion channel (especially if it is specific to

axons), would be desirable here, and a clearer understanding of the human axonal K^+ channel population is a necessary step in this direction.

Baker, M., Bostock, H., Grafe, P. & Martius, P. (1987). Function and distribution of three types of rectifying channel in rat spinal root myelinated axons. *Journal of Physiology* **383**, 45–67.

Baukrowitz, T. & Yellen, G. (1995). Modulation of K^+ current by frequency and external $[K^+]$: a tale of two inactivation mechanisms. *Neuron* **15**, 951–960.

Bostock, H. & Baker, M. (1988). Evidence for two types of potassium channel in human motor axons *in vivo*. *Brain Research* **462**, 354–358.

Chiu, S. Y., Ritchie, J. M., Rogart, R. B. & Stagg, D. (1979). A quantitative description of membrane currents in rabbit myelinated nerve. *Journal of Physiology* **292**, 149–166.

Chung, S. & Kaczmarek, L. K. (1995). Modulation of the inactivation of voltage-dependent potassium channels by cAMP. *Journal of Neuroscience* **15**, 3927–3935.

Colquhoun, D. & Hawkes, A. G. (1983). The principles of the stochastic interpretation of ion-channel mechanisms. In *Single-Channel Recording*, ed. Sakmann, B. & Neher, E., pp. 135–175. Plenum Press, New York.

Corey, D. P. & Stevens, C. F. (1983). Science and technology of patch-recording electrodes. In *Single-Channel Recording*, ed. Sakmann, B. & Neher, E., pp. 53–68. Plenum Press, New York.

Corrette, B. J., Repp, H., Dreyer, F. & Schwarz, J. R. (1991). Two types of fast K^+ channels in rat myelinated nerve fibres and their sensitivity to dendrotoxin. *Pflügers Archiv* **418**, 408–416.

Davis, F. A., Stefoski, D. & Rush, J. (1990). Orally administered 4-aminopyridine improves clinical signs in multiple sclerosis. *Annals of Neurology* **27**, 186–192.

Demo, S. D. & Yellen, G. (1991). The inactivation gate of the *Shaker* K^+ channel behaves like an open-channel blocker. *Neuron* **7**, 743–753.

Dubois, J. M. (1981). Evidence for the existence of three types of potassium channels in the frog Ranvier node membrane. *Journal of Physiology* **318**, 297–316.

Durham, A. C. H. (1983). A survey of readily available chelators for buffering calcium ion concentrations in physiological solutions. *Cell Calcium* **4**, 33–46.

Gold, M. S., Shuster, M. J. & Levine, J. D. (1996). Characterization of six voltage gated K^+ currents in adult rat sensory neurons. *Journal of Neurophysiology* **75**, 2629–2646.

Grafe, P., Bostock, H. & Schneider, U. (1994). The effects of hyperglycaemic hypoxia on rectification in rat dorsal root axons. *Journal of Physiology* **480**, 297–307.

Grissmer, S. (1986). Properties of potassium and sodium channels in frog internode. *Journal of Physiology* **381**, 119–134.

Hamill, O. P., Marty, A., Neher, E., Sakmann, B. & Sigworth, F. J. (1981). Improved patch-clamp techniques for high-resolution current recording from cells and cell-free membrane patches. *Pflügers Archiv* **391**, 85–100.

Harrison, S. M. & Bers, D. M. (1989). Correction of proton and Ca association constants of EGTA for temperature and ionic strength. *American Journal of Physiology* **256**, C1250–1256.

Inglis, J. T., Leeper, J. B., Wilson, L. R., Gandevia, S. C. & Burke, D. (1998). The development of conduction block in single human axons following a focal nerve injury. *Journal of Physiology* **513**, 127–133.

Jonas, P., Bräu, M. E., Hermsteiner, M. & Vogel, W. (1989). Single-channel recording in myelinated nerve fibers reveals one type of Na channel but different K channels. *Proceedings of the National Academy of Sciences of the USA* **86**, 7238–7242.

Koh, D.-S. & Vogel, W. (1996). Single-channel analysis of a delayed rectifier K^+ channel in *Xenopus* myelinated nerve. *Journal of Membrane Biology* **149**, 221–232.

Marty, A. & Neher, E. (1995). Tight-seal whole-cell recording. In *Single-Channel Recording*, 2nd edn, ed. Sakmann, B. & Neher, E., pp. 31–52. Plenum Press, New York.

Miller, D. J. & Smith, G. L. (1984). EGTA purity and the buffering of calcium ions in physiological solutions. *American Journal of Physiology* **246**, C160–166.

Poulter, M. O., Hashiguchi, T. & Padjen, A. L. (1989). Dendrotoxin blocks accommodation in frog myelinated axons. *Journal of Neurophysiology* **62**, 174–184.

Rasmusson, R. L., Morales, M. J., Castellino, R. C., Zhang, Y., Campbell, D. L. & Strauss, H. C. (1995). C-type inactivation controls recovery in a fast inactivating cardiac K^+ channel (Kv1.4) expressed in *Xenopus* oocytes. *Journal of Physiology* **489**, 709–721.

Reid, G. (1993). A disposable, small volume solution changer for isolated patch recording. *Journal of Physiology* **459**, 121*P*.

Robertson, B. (1997). The real life of voltage-gated K^+ channels: more than model behaviour. *Trends in Pharmacological Sciences* **18**, 474–483.

Röper, J. & Schwarz, J. R. (1989). Heterogeneous distribution of fast and slow potassium channels in myelinated rat nerve fibres. *Journal of Physiology* **416**, 93–110.

Safronov, B. V., Bischoff, U. & Vogel, W. (1996). Single voltage-gated K^+ channels and their functions in small dorsal root ganglion neurones of rat. *Journal of Physiology* **493**, 393–408.

Safronov, B. V., Kampe, K. & Vogel, W. (1993). Single voltage-dependent potassium channels in rat peripheral nerve membrane. *Journal of Physiology* **460**, 675–691.

Schneider, U., Quasthoff, S., Mitrović, N. & Grafe, P. (1993). Hyperglycaemic hypoxia alters after-potential and fast K^+ conductance of rat axons by cytoplasmic acidification. *Journal of Physiology* **465**, 679–697.

Scholz, A., Reid, G., Vogel, W. & Bostock, H. (1993). Ion channels in human axons. *Journal of Neurophysiology* **70**, 1274–1279.

Schwarz, J., Reid, G. & Bostock, H. (1995). Action potentials and membrane currents in the human node of Ranvier. *Pflügers Archiv* **430**, 283–292.

Schwarz, J. R. & Vogel, W. (1971). Potassium inactivation in single myelinated nerve fibres of *Xenopus laevis*. *Pflügers Archiv* **330**, 61–73.

Schwid, S. R., Petrie, M. D., McDermott, M. P., Tierney, D. S., Mason, D. H. & Goodman, A. D. (1997). Quantitative assessment of sustained-release 4-aminopyridine for symptomatic treatment of multiple sclerosis. *Neurology* **48**, 817–821.

Sunderland, S. (1968). *Nerves and Nerve Injuries*. E & S Livingstone, Edinburgh.

Vogel, W. & Schwarz, J. R. (1995). Voltage-clamp studies in axons: macroscopic and single-channel currents. In *The Axon*, ed. Waxman, S. G., Kocsis, J. D. & Stys, P. K., pp. 257–280. Oxford University Press, Oxford.

Wang, H., Kunkel, D. D., Martin, T. M., Schwartzkroin, P. A. & Tempel, B. L. (1993). Heteromultimeric K^+ channels in terminal and juxtaparanodal regions of neurons. *Nature* **365**, 75–79.

Wilson, G. F. & Chiu, S. Y. (1990). Ion channels in axon and Schwann cell membranes at paranodes of mammalian myelinated fibers studied with patch clamp. *Journal of Neuroscience* **10**, 3263–3274.

Acknowledgements

We are grateful to Mr Rolfe Birch, Consultant Orthopaedic Surgeon, Royal National Orthopaedic Hospital for the human nerve graft material and to Pfizer UK Ltd for paying for its delivery by courier. This study was supported financially by the Medical Research Council, the British Council and the Deutsche Akademische Austauschdienst.

Corresponding author

G. Reid: Department of Animal Physiology and Biophysics, Faculty of Biology, University of Bucharest, Splaiul Independentei 91–95, Bucharest 76201, Romania.

Email: gordon@bio.bio.unibuc.ro